HHS Public Access

Author manuscript

ACS Appl Bio Mater. Author manuscript; available in PMC 2021 June 11.

Published in final edited form as:

ACS Appl Bio Mater. 2020 April 20; 3(4): 1976–1985. doi:10.1021/acsabm.9b01141.

Nanoparticle Delivery of CD147 Antagonistic Peptide-9 Protects against Acute Ischemic Brain Injury and tPA-Induced Intracerebral Hemorrhage in Mice

Shan Liu, **Rong Jin**, **Min Wang**, **Guohong Li**

Department of Neurosurgery, The Pennsylvania State, University College of Medicine, Hershey, Pennsylvania 17033, United States

Abstract

CD147 has emerged as a potential therapeutic target in many human diseases. We have demonstrated that inhibition of CD147 using its function-blocking antibody ameliorates acute ischemic brain injury and promotes long-term functional recovery in mice. Recently, peptide–nanoparticle conjugates have emerged as powerful tools for biomedical applications. The present study aimed to investigate the therapeutic potential of CD147 antagonist peptide-9 (AP9) in acute ischemic stroke in mice using nanomaterial as the drug delivery vehicles. AP9-conjugated nanoparticles (APN), with an average size of about 40 nm, were fabricated by maleimide linkage and characterized using dynamic light scattering and transmission electron microscopy. We found that APN specifically bound to CD147 in cultured mouse brain endothelial cells (bEnd.3) and to ischemia-induced CD147 in mouse cerebral microvessels. Using a mouse model of transient middle cerebral artery occlusion (tMCAO), we demonstrated, for the first time, that systemic delivery of APN (2.5 mg/kg, I.V.) initiated at 1 h after tMCAO significantly reduced brain infarct size, improved functional outcome, and attenuated delayed (5 h after tMCAO) tPA-induced intracerebral hemorrhage in acute ischemic stroke. These protective effects were associated with profound inhibition of MMP-9 and MMP-3 in both ischemic brain and plasma. In conclusion, the CD147 antagonist peptide-9 represents a potentially promising therapeutic candidate for the treatment of ischemic stroke.

Graphical Abstract

Corresponding Author: Guohong Li – Department of Neurosurgery, The Pennsylvania State University College of Medicine, Hershey, Pennsylvania 17033, United States; guohongli@pennstatehealth.psu.edu.

Author Contributions

S.L., R.J., and M.W. performed experiments and data analysis. S.L. wrote the manuscript. G.L. designed and supervised the study and revised the manuscript.

Supporting Information

The Supporting Information is available free of charge at https://pubs.acs.org/doi/10.1021/acsabm.9b01141.

Infarct volumes, TTC stain, mice, systemic administration, naked AP9 (PDF)

The authors declare no competing financial interest.

Complete contact information is available at: https://pubs.acs.org/10.1021/acsabm.9b01141

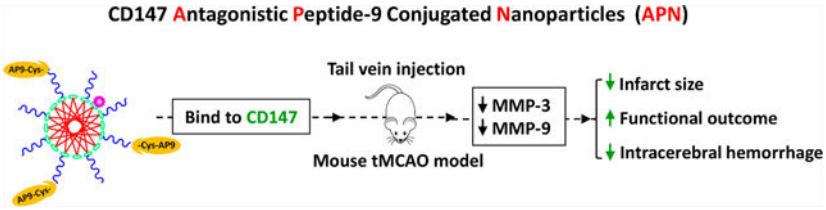

Keywords

CD147; antagonistic peptide; peptide-conjugated nanoparticles; ischemic stroke; matrix metalloproteinases; middle cerebral artery occlusion

INTRODUCTION

Ischemic stroke is a cerebrovascular disease that results from the temporary or permanent occlusion of vital cerebral arteries. To date, intravenous administration of tPA (tissue-type plasminogen activator; IV tPA) remains the only Food and Drug Administration-approved drug therapy for achieving cerebral reperfusion. However, only very limited stroke cases (3% to 8.5%) benefit from IV tPA due to its narrow therapeutic window (within 4.5 h of stroke onset) and the increased risks of fatal intracranial hemorrhage.[1] Therefore, there is a pressing need for developing new treatment strategies to combat cerebral ischemia, the leading cause of disability and mortality worldwide. Accumulating evidence suggests that biomolecular drugs, including peptides and proteins, are promising for the treatment of ischemic stroke.[2–4] However, the inherent instability in plasma and the low penetration through the blood–brain barrier (BBB) of biomolecular drugs usually hamper their further clinical translation. Recently, nanotechnology has emerged as a promising strategy to enhance the in vivo stability and achieve the CNS availability of therapeutic biomolecules.[5,6]

CD147 (cluster of differentiation 147), a cell surface glycoprotein of the IgG superfamily, servers as a potent inducer of extracellular matrix metalloproteinases (MMPs) and modulates the synthesis and activity of MMPs.[7] Increased expression of CD147 has been implicated in many human diseases including cancer, cardiovascular diseases, and neurological disorders.[8] It has been demonstrated in patients and experimental stroke models that cerebral ischemia significantly induces CD147 expression.[9–13] Moreover, the increase in CD147 following cerebral ischemia plays a key role in regulating MMPs activities, and mediates the pathology of ischemic injury, including stroke-induced BBB dysfunction, microvascular thrombosis, cerebral inflammation, and pneumonia.[10–12] Our previous studies have shown that ischemia-induced CD147 expression substantially contributes to stroke-associated pneumonia, acute ischemic brain injury, and long-term white matter damage and functional impairment after ischemic stroke in mice.[8,12,13] Our findings suggest making CD147 a promising target for therapeutic intervention in cerebral ischemia.

Antagonistic peptide-9 (AP9), a CD147 antagonistic peptide, binds specifically to CD147 and significantly inhibits the function of CD147 in tumor cell lines.[14] Therapeutic targeting of CD147 using AP9 has been shown to prevent cancer invasion and metastasis.[14,15] Besides the widely validated efficacy of AP9 in various cancers, one recent study demonstrated that

AP9 attenuates ischemic/reperfusion injury in an experimental model of acute myocardial infarction.[16] Considering that CD147 is recognized as a substantial contributor to the evolution of ischemic injury and behavioral deficit after stroke,[8,12] we hypothesized that targeting CD147 using AP9 may functionally antagonize CD147 and thus provide protective effects on ischemic stroke. In this study, we aimed to assess the therapeutic potential of AP9 in acute ischemic stroke in mice using nanomaterial as the drug delivery tool. As a CD147 antagonistic peptide, AP9 inhibits the dimerization of CD147[17] as well as the CD147-cyclophilin A interaction,[17,18] and both can mediate the induction of MMPs.[7,18] In the present study, we investigated the role and the possible mechanisms of action of nanoparticle-delivered CD147 antagonistic peptide-9 in ischemic stroke in mice.

EXPERIMENTAL SECTION

Materials and Reagents.

DSPE (1, 2-distearoyl-*sn*-glycero-3-phosphorylethanolamine), DSPE-PEG(2000), DSPE-PEG(2000)-maleimide, and DSPE-rhodamine were purchased from Avanti polar lipids (Alabaster, AL). Cysteine modified AP-9 peptide (Cys-YKLPGHHHHYRP) and scrambled AP-9 peptide (Cys-HYLPGHRHPYHK) were synthesized by GenScript (Piscataway, NJ). Other chemicals with high-grade purity were obtained from Thermo Fisher Scientific.

Preparation of Polymeric Nanoparticle.

DSPE, DSPE-PEG_{2000}, DSPE-rhodamine, and DSPE-PEG_{2000}-maleimide, in a molar ratio of 50:39:10:1, were dissolved in 20 mL solvent of chloroform/methanol (4:1, V/V). After evaporating, the obtained thin and uniform lipid film was hydrated with 6 mL of HEPES buffer (0.01M, pH 6.5) for 1 h at 60 °C, cooled at room temperature, and then placed at 4 °C for 30 min. The C-terminal cysteine residue-modified AP9 (Cys-AP9) or scrambled AP9 (Cys-SC-AP9) mixed with DSPE-PEG_{2000}-maleimide in a molar ratio of 1.5 to 1 was added to the cooled hydrated aqueous solution and reacted under nitrogen at 4 °C overnight (about 12 h). The reaction mixture was then concentrated using centrifugal concentrator (100 K COMW, Corning) at 3000*g* for four cycles (20 min each) to remove unconjugated Cys-AP9 or Cys-SC-AP9, and the concentration of unconjugated Cys-AP9 or Cys-scram-AP9 in the supernatant was measured by high performance liquid chromatography (HLPC). The obtained AP9 or SC-AP9-nanoparticle conjugates (namely APN and SAPN, respectively) were diluted with HEPES buffer to yield a final concentration of about 1 mg/mL (corresponding to a concentration of 608 μM, AP9/SC-AP9 molecular weight: 1645).

Dynamic Light Scattering and Zeta Potential.

Particle size distribution and zeta potential of APN or SAPN were determined as described previously using a ZETA-SIZER Nano-ZS (Malvern Instruments, Ltd., UK) at 25 °C.[19] APN or SAPN stock solution (1 mg/mL corresponding to AP9 or SC-AP9) was diluted at 1:100 with HEPES buffer (0.01M, pH 6.5) before measurement. Each measurement was performed in triplicate.

Morphology by Transmission Electron Microscopy (TEM).

The morphology of APN was characterized using a transmission electron microscope (Hitachi H-7650, Japan) after dilution at 1:100 with HEPES buffer (0.01M, pH 6.5), as described previously.[20]

Blood Compatibility.

Blood compatibility was evaluated with hemolysis assay as described previously.[21] Freshly isolated mouse red blood cells (RBCs) were incubated with AP9-conjugated nanoparticles (APN) at final concentration range of 0.01–100 μM or blank nanoparticles only (BLANK) for 1 h at 37 °C in Dulbecco's PBS (D-PBS). After centrifugation (700*g* for 10 min at 4 °C), the hemoglobin absorbance of the all the supernatant was measured at 577 nm with the 655 nm as a reference by a microplate reader (Molecular Devices, USA). RBCs incubated with distilled water and D-PBS were used as positive and negative controls, respectively. Experiments were performed in triplicate. The hemolytic degree was expressed by the hemolytic ratio calculated according to the following formula:

$$\text{hemolysis ratio} = \left(\text{OD}_{\text{test}} - \text{OD}_{\text{negative control}}\right) / \left(\text{OD}_{\text{positive control}} - \text{OD}_{\text{negative control}}\right) \times 100$$

Cytotoxicity and In Vivo Toxicity.

To investigate the cytotoxicity of AP9, scrambled AP9, AP9-conjugated nanoparticles (APN), scramble AP9-conjugated nanoparticles (SAPN), and blank nanoparticles (BLKN, without AP9 or scramble AP9), we conducted 3-(4, 5-dimethyl-2-thiazolyl)-2, 5-diphenyl-2H tetrazolium bromide (MTT) assay as described previously using bEnd.3 (ATCC CRL-2299) and CATH.a (ATCC CRL-11179) cell lines.[20] bEnd.3 is a mouse brain endothelial cell line, and CATH.a is a mouse brain neuron cell line. Both cell lines were purchased from American Type Culture Collection (ATCC).

In vivo toxicity was evaluated in healthy mice 3 days after intravenous injection of APN or SAPN at the dose of 5 mg/kg using HE staining of primary organs (heart, liver, spleen, lung, kidney, and brain).

Mouse Stroke Model and Drug Treatment.

Focal cerebral ischemia was induced in C57BL/6 mice (8–10 weeks, Jackson Laboratories, Bar Harbor, ME) by a 60 min transient middle cerebral artery (MCA) occlusion (tMCAO) using the intraluminal filament occlusion method as we described previously.[8,12] Briefly, a 6–0 silicone-coated nylon monofilament (Doccol Corp.) was introduced from the left external carotid artery into the internal carotid artery and advancing it to the origin of the MCA until cerebral blood flow was abruptly reduced. After 60 min of the occlusion, the restoration of blood flow to the MCA territory is made by withdrawal of the nylon suture. Sham-operated animals underwent anesthesia and exposure of the arteries without MCA occlusion.

After surgery, the mice were randomly divided into three treatment groups: APN, SAPN, or saline vehicle. APN or SAPN (the stock solution in HEPES buffer: 1 mg/mL corresponding to AP9 or SC-AP9) was diluted to the desired concentrations using normal saline and administrated via tail vein injection in a total volume of 100 μL initiated at 1 h after induction of tMCAO.

Affinity of APN and SAPN to CD147 In Vitro and In Vivo.

To measure the in vitro affinity of APN and SAPN to CD147, bEnd.3 cells were seeded on the coverslips in a 24-well plate. When the cells formed confluent monolayers, the previous medium was removed, and they were washed thrice with PBS and then incubated with serum-free medium containing Rhodamine-labeled APN or SAPN (10 nM) for 1 h. After that, cells were washed twice with PBS, fixed with 2% PFA in PBS solution, immunostained for CD147 (1:200, Abcam), and visualized by fluorescence microscopy.

To test the in vivo affinity of APN and SAPN to CD147, both normal mice and tMCAO mice were injected with Rhodamine-labeled APN or SAPN solution (corresponding to AP9 of 2.5 mg/kg body weight, and rhodamine of 15 μmol/kg body weight) at 1 h after tMCAO onset. After transcardial perfusion with cold PBS (pH 7.4) under deep anesthesia at 4 h after induction of tMCAO, brains were immediately removed, fixed in 4% paraformaldehyde overnight, rinsed several times in PBS, then stored in 30% sucrose at 4 °C until the brains sank. Brains were embedded in optimal cutting temperature compound (OCT compound) prior to frozen sectioning to 6 μm thick coronal sections. Sections were further immunostained for CD147 (1:200; Abcam) as we described previously.[12]

Infarct Volume, Intracerebral Hemorrhage, and Neurological Deficits.

Mice were euthanized at 3 days after tMCAO. After transcardial perfusion with 30 mL of normal saline, brains were removed and cut into seven 1 mm-thick coronal sections. The brain sections were stained with 2% 2,3,5-triphenyltetrazolium chloride (TTC) for 10 min. Infarct volume was determined on TTC-stained sections using Image-Pro Plus software (version 6.0). In TTC staining, viable tissue is stained red, and lack of TTC staining (white) is considered “infarcted”.[22] The actual infarct volume corrected with edema was calculated as we described previously.[23] The modified Bederson score[24] and the grip strength test[25] were assessed in a blind manner before and at 3 days after tMCAO as described.[12] Hemoglobin levels were measured in the TTC-stained sections by a spectrophotometric assay using Drabkin reagent (Sigma-Aldrich).[26]

Western Blot and Gelatin Zymography.

Proteins were extracted from the cerebral cortices (bregma +2 to −3 mm) and the plasma 24 h after stroke. The two assays were conducted as described.[23,27] The following primary antibodies were used for Western blotting: MMP-3 (1:1000; Abcam); β-actin (1:1000; Sigma); transferrin (1:1000; Abcam). Semiquantitative assessment of immunoblots and MMP bands was performed by computerized densitometry.

Statistics.

Data are expressed as mean ± standard deviation. Graph Pad Prism 5 software was used for statistical analysis. One-way ANOVA followed by the Bonferroni post hoc test, and two-tailed Student's *t* test were used to determine significant differences among multiple groups and between two groups, respectively. $P < 0.05$ was considered statistically significant.

RESULTS

Fabrication and Characterizations of AP9 Peptide–Nanoparticle Conjugates.

The AP9 peptide–nanoparticle conjugates (APN) were prepared using film dispersion method. APN was fabricated by the bioconjugation of cysteine-modified CD147-antagonistic peptide 9 (Cys-AP9) to the maleimide moieties of polymeric nanoparticles (DSPE-PEG-maleimide),[23] as illustrated in Figure 1A. SAPN was generated by cysteine-modified AP-9 scrambled peptide (Cys-SC-AP9) and conjugated similarly as APN. The size distribution and morphology of the APN were determined using dynamic light scattering (DLS) method and transmission electron microscopy (TEM), respectively. As shown in Figure 1B and C, APN showed an average diameter of $D = 38.71 \pm 0.81$ nm and a zeta potential of $\zeta = -20.93 \pm 0.97$ mV. TEM image (Figure 1D) confirms that APN featured nanostructures with a size of about 40 nm.

The blood compatibility, cytotoxicity, and in vivo toxicity of APN were evaluated by hemolysis analysis, MTT cell viability assay, and HE staining of primary organs, respectively. Hemolysis assay demonstrated that both blank nanoparticles (BLKN, without AP9 or scramble AP9) and APN showed superior blood compatibility even at concentration as high as 100 μM (Figure 2A,B). The in vitro cytotoxicity of APN was assessed by MTT in both mouse brain endothelial cell line (bEnd.3) and mouse brain neuron cell line (CATH.a), and neither bEnd.3 nor CATH.a cells showed significant cell toxicity when treated with different concentrations of APN (1, 10, and 100 nM) (Figure 2C,D). APN and SAPN at 1000 nM showed moderate cytotoxicity to both bEnd.3 nor CATH.a cells, which is due to the cytotoxicity of blank PN (BLKN), as both Cys-AP9 and Cys-SAP9 had no cell toxicity, whereas BLKN showed similar cytotoxicity at 1000 nM. HE staining images of the primary organs from mice 3 days after APN injection showed no appreciable abnormality or noticeable organ damage (Figure 2E), suggesting no detectable in vivo acute toxicity.

APN Binds Specifically to CD147 In Vitro and In Vivo.

Specific binding of targeted APN to endogenous CD147 was investigated in vitro using bEnd.3 mouse brain endothelial cells and in vivo using transient MCAO (tMCAO) model in mice. bEnd.3 cells were incubated with rhodamine-labeled APN (Rho-APN, corresponding to 10 nM AP9) for 1 h, then further immunostained for CD147. We found that Rho-APN bound specifically to endogenous CD147 in bEnd.3 cells, as revealed by the extensive colocalization of Rho-APN with CD147 as shown in Figure 3A. However, SAPN, which is fabricated with scrambled AP9, showed minimal binding affinity to endogenous CD147 (Figure 3A).

Our previous data demonstrated that CD147 is minimally expressed in normal brain microvessels, but its expression significantly and rapidly increased in brain microvessels as early as 4 h after tMCAO in mice.[12] Here, we found that APN bound barely to normal brain microvessels but abundantly to ischemic microvessels 4 h after stroke (Figure 3B) due to the increased CD147 expression in the ischemic brain endothelium. SAPN showed almost no binding to microvessels in either normal or ischemic brains (Figure 3B), as expected. Double immunostaining further confirmed the in vivo binding of APN with ischemia-induced CD147 in CD31-positive microvascular endothelial cells (Figure 3C–E).

APN Improves Acute Stroke Outcome and Reduces tPA-Induced Intracerebral Hemorrhage.

Acute stroke outcome was evaluated on day 3 after stroke. Significantly reduced infarct volumes were observed in mice administrated intravenously with APN at doses of 2.5 to 5 mg/kg initiated at 1 h after tMCAO ($P < 0.01$), whereas a lower dose of 0.5 mg/kg APN showed no significant effect compared with mice administrated with vehicle (Figure 4A,B). No significant difference in infarct volumes was found between mice treated with 2.5 mg/kg SAPN and vehicle (Figure 4A,B). Functionally, the smaller infarct volumes correlate positively to better neurological outcome. Mice administrated with APN (2.5 or 5 mg/kg) showed significant improvement in overall neurological function (Figure 4C) and motor function and coordination (Figure 4D) compared with vehicle control. On the basis of these data, the dose 2.5 mg/kg of APN or SAPN was used for further experiments.

Intracerebral hemorrhage (ICH) was evaluated on day 1 after stroke. Delayed IV tPA (10 mg/kg, 10% as bolus and remaining as infusion over 30 min) was administrated at 5 h after tMCAO to induce ICH in mice.[28] We found here that APN, but not SAPN, at a dose of 2.5 mg/kg initiated at 1 h after tMCAO significantly reduced delayed tPA-associated ICH 24h after tMCAO in mice (Figure 4E).

APN Reduces Activity/Expression of Ischemia-Induced Cerebral and Plasma MMPs.

MMPs (matrix metalloproteinases), in particular MMP-9, are significantly increased by cerebral ischemia and play a pivotal role in brain damage and tPA-associated hemorrhage after stroke.[26,29] Gelatin zymography was performed to assess MMP-2/MMP-9 activities in the cerebral cortex and plasma at 24 h after stroke. As expected, both cerebral MMP-2/MMP-9 enzyme activities were low at baseline in Sham control (Figure 5A). APN, but not SAPN, significantly inhibited ischemia-induced MMP-9 and MMP-2 in the ischemic brain (Figure 5A). APN also inhibited the increased activity of MMP-9 in plasma, whereas plasma MMP-2 activity was not altered by either APN or SAPN (Figure 5B). In addition to increased activity of MMP-2/MMP-9, expressions of MMP-3 in both the cerebral cortex and plasma were dramatically decreased after APN treatment (Figure 5C) 24 h after stroke, as detected by Western blotting.

DISCUSSION

In this study, we fabricated and characterized CD147 antagonistic peptide-conjugated nanoparticles (APN) and demonstrated, for the first time, its efficacy in reducing brain

infarct size, improving functional outcome, and attenuating tPA-induced intracerebral hemorrhage in the tMCAO mouse ischemic model. Mechanistically, we provided evidence showing that the protective effects of APN were associated with profound inhibition of MMP-9 and MMP-3 in both ischemic brain and plasma.

Peptides represent a unique class of pharmaceutical compounds, which exhibit target specificity (protein functionalities) and low inherent toxicity, and possess a high degree of modularity in molecular design.[30] Accumulating studies have demonstrated the effectiveness of different therapeutic peptides in ischemia stroke in attenuating neuronal apoptosis,[31,32] inhibiting inflammatory,[33] targeting oxidative stress,[34] and promoting angiogenesis.[35] However, to overcome the inherent low in vivo stability and weak CNS availability of these peptides, various strategies have been utilized including customized synthetic methods, specialized administration routes (intranasal delivery; intracerebroventricular injection), conjugation to carrier molecules (e.g., cell-penetrating peptide), or delivery in nanoparticles (e.g., hydrogels, liposomes). In this study, we fabricated APN by conjugating CD147 antagonistic peptide (AP9) to polymeric nanoparticles using maleimide linkage, a technique that is widely applied in clinically approved antibody–drug conjugates.[36] We found that APN bound efficiently to ischemia-induced CD147 in mouse cerebral microvessels within the ipsilateral hemisphere after ischemic stroke, suggesting that APN achieved the successful delivery of AP9 to brain after systemic administration. We also found partial penetration of APN in the ischemic parenchyma, which is likely due to the enhanced transvascular transport enabled by lipid-based nanocarriers and the compromised BBB integrity following ischemia as well. Our previous study demonstrated that ischemia-induced CD147 expressed mainly in CD31-positive microvascular endothelial cells but rarely in other brain parenchyma cells (astrocytes, microglia, and neurons) in the acute phase (4–24 h) of tMCAO.[12] Therefore, the observed binding of APN is prominently limited to microvascular endothelial cells. Notably, we provided strong, albeit indirect, evidence showing that APN greatly reserved the bioactivity of AP9 during circulation. This is supported by the following findings: (1) APN showed significant stronger binding with the cerebral microvessels and higher penetration into the ischemic parenchyma in comparison with SAPN; (2) APN at dose of 2.5 mg/kg dramatically reduced infarct volumes, whereas systemic administration of naked AP9 at dose of up to 5 mg/kg showed no significant effects in reducing infarct volumes (Figure S1). Taken together, APN improved the brain penetration and in vivo bioactivity of AP9, and peptide–nanoparticle conjugates showed great promise for the delivery of therapeutic biomolecules in ischemic stroke management. Nevertheless, the biosafety of the in vivo application of nanomaterials warrants further investigation.

CD147, a well-established anticancer target,[37,38] recently emerges as a potential therapeutic target for cerebral ischemia. To date, a variety of CD147 targeting strategies have been validated including small interfering RNA,[39,40] antibodies (Licartin; CNTO 3899),[38,40,41] peptides,[14,16] and small-molecule compound (AC-73; SP-8356).[42–44] These various CD147 targeting strategies were predominantly evaluated in cancer therapy with respect to blocking the cancer-related functions of CD147, with few antibodies tested in cerebral ischemia and only one peptide tested in myocardial ischemia.[8,12,13,16] Our previous studies demonstrated the effectiveness of anti-CD147 function-blocking antibody (αCD147) in both the acute and

recovery phase of ischemic stroke in mouse.[8,12,13] Herein, we employed a CD147 antagonistic peptide (AP9) to therapeutically target CD147 and demonstrated its protective effects in tMCAO mouse ischemic model. Notably, we found that AP9 significantly ameliorated delayed tPA-induced intracerebral hemorrhage (ICH), suggesting that AP9 may be a potential adjuvant for IV tPA to reduce the risks of ICH by late thrombolytic therapy of IV tPA and provide neuroprotective effects as well. Moreover, targeting CD147 using peptides may show great advantage over antibodies regarding to clinical translation potential because clinical translation of therapeutic antibodies is facing several limitations including immune cross reactivity, antibody-mediated side effects, and high production costs.[45,46] Therefore, our findings here suggest that CD147 antagonistic peptide (AP9) represents a potentially promising therapeutic candidate for the treatment of ischemic stroke.

We demonstrated here that systemic delivery of APN inhibited the cerebral and plasma MMP-9/MMP-3/MMP-2 in the acute phase (24 h) of ischemic stroke, leading to improved acute stroke outcome and reduced delayed-tPA-induced intracerebral hemorrhage (ICH). AP9 antagonizes CD147 through disrupting its dimerization, thereby inhibiting the induction of CD147 downstream MMPs.[7,17,18] In this regard, the previously validated in vitro anticancer activities and in vivo protective effects in acute myocardial ischemia of AP9 are attributed to inhibiting the expression/activation of MMP-2/MMP-9.[14–17] Consistently, we demonstrated here that targeting CD147 using AP9 inhibited the activity/expression of both cerebral and plasma MMP-9/MMP-3 and activity of cerebral MMP-2. It has been well documented that MMPs, mainly the constitutive MMP-2 and inducible MMP-3/MMP9, are activated in response to ischemia and play important roles in infarction progression and pathogenesis of ischemic-stroke-associated ICH by causing the disruption of vasculature.[47,48] Moreover, clinical data have shown that high plasma levels of MMP-9 in the acute phase of a cerebral infarct are independent predictors of ICH in all stroke subtypes.[49] Therefore, the reduced cerebral and plasma MMPs observed in this study most likely contributed to the decreased infarct sizes, improved functional outcome, and attenuated delayed-IV tPA-associated ICH, but the exact mechanism needs further investigation. Especially, in addition to the well-documented inhibition of MMP-2/MMP-9 by AP9, this study provided the first direct evidence showing that AP9 inhibited the activity/expression of cerebral/plasma MMP-3. This previously undescribed role of AP9 in inhibiting MMP-3 is supposed to be critical for reducing tPA-associated ICH, as MMP-3 is relatively more important than MMP-9 for the tPA-reduced IHC in ischemic stroke.[50,51] This finding provided evidence supporting AP9 as a potential adjuvant for IV tPA thrombolytic therapy in ischemic stroke.

CONCLUSION

In summary, pharmacological inhibition of CD147 using its antagonistic peptide (AP9) improves acute stroke outcome and reduces delayed tPA-induced intracerebral hemorrhage through modulating the cerebral and plasma MMPs. This preliminary study also highlights that peptide–nanoparticle conjugates are powerful tools for the successful in vivo applications of therapeutic biomolecules in ischemic stroke therapy.

Supplementary Material

Refer to Web version on PubMed Central for supplementary material.

Funding

This work was supported by National Institutes of Health Grant Nos. NS088719 and NS089991 (G.L.).

REFERENCES

(1). Bambauer KZ; Johnston SC; Bambauer DE; Zivin JA Reasons why few patients with acute stroke receive tissue plasminogen activator. Arch. Neurol 2006, 63 (5), 661–4. [PubMed: 16682535]

(2). Lyden P; Pryor KE; Coffey CS; Cudkowicz M; Conwit R; Jadhav A; Sawyer RN; Claassen J; Adeoye O; Song S; Hannon P; Rost NS; Hinduja A; Torbey M; Lee JM; Benesch C; Rippee M; Rymer M; Froehler MT; Clarke Haley E; Johnson M; Yankey J; Magee K; Qidwai J; Levy H; Mark Haacke E; Fawaz M; Davis TP; Toga AW; Griffin JH; Zlokovic BV; Investigators NCTNN Final Results of the RHAPSODY Trial: A Multi-Center, Phase 2 Trial Using a Continual Reassessment Method to Determine the Safety and Tolerability of 3K3A-APC, A Recombinant Variant of Human Activated Protein C, in Combination with Tissue Plasminogen Activator, Mechanical Thrombectomy or both in Moderate to Severe Acute Ischemic Stroke. Ann. Neurol 2019, 85 (1), 125–136. [PubMed: 30450637]

(3). Hill MD; Martin RH; Mikulis D; Wong JH; Silver FL; Terbrugge KG; Milot G; Clark WM; Macdonald RL; Kelly ME; Boulton M; Fleetwood I; McDougall C; Gunnarsson T; Chow M; Lum C; Dodd R; Poublanc J; Krings T; Demchuk AM; Goyal M; Anderson R; Bishop J; Garman D; Tymianski M; Investigators, E. t. Safety and efficacy of NA-1 in patients with iatrogenic stroke after endovascular aneurysm repair (ENACT): a phase 2, randomised, double-blind, placebo-controlled trial. Lancet Neurol. 2012, 11 (11), 942–50. [PubMed: 23051991]

(4). Reis C; Akyol O; Ho WM; Araujo C; Huang L; Applegate R; Zhang JH Phase I and Phase II Therapies for Acute Ischemic Stroke: An Update on Currently Studied Drugs in Clinical Research. BioMed Res. Int 2017, 2017, 4863079. [PubMed: 28286764]

(5). Liu S; Feng X; Jin R; Li G Tissue plasminogen activator-based nanothrombolysis for ischemic stroke. Expert Opin. Drug Delivery 2018, 15 (2), 173–184.

(6). Bonnard T; Gauberti M; Martinez de Lizarrondo S; Campos F; Vivien D Recent Advances in Nanomedicine for Ischemic and Hemorrhagic Stroke. Stroke 2019, 50 (5), 1318–1324. [PubMed: 30932782]

(7). Grass GD; Toole BP How, with whom and when: an overview of CD147-mediated regulatory networks influencing matrix metalloproteinase activity. Biosci. Rep 2016, 36 (1), No. e00283.

(8). Liu S; Jin R; Xiao AY; Zhong W; Li G Inhibition of CD147 improves oligodendrogenesis and promotes white matter integrity and functional recovery in mice after ischemic stroke. Brain, Behav., Immun 2019, 82, 13–24. [PubMed: 31356925]

(9). Xu B; Wu C; Wu W; Tan Y; Sun N; Cui J; Lu S; Wang J; Cen S Study of Serum CD147 Level in Patients with Transient Ischemic Attack and CD147 Expression in Atherosclerotic Plaque. J. Cardiovasc Transl Res 2018, 11 (4), 285–291. [PubMed: 30039437]

(10). Burggraf D; Liebetrau M; Martens HK; Wunderlich N; Jäger G; Dichgans M; Hamann GF Matrix metalloproteinase induction by EMMPRIN in experimental focal cerebral ischemia. Eur. J. Neurosci 2005, 22 (1), 273–7. [PubMed: 16029217]

(11). Zhu W; Khachi S; Hao Q; Shen F; Young WL; Yang GY; Chen Y Upregulation of EMMPRIN after permanent focal cerebral ischemia. Neurochem. Int 2008, 52 (6), 1086–91. [PubMed: 18164515]

(12). Jin R; Xiao AY; Chen R; Granger DN; Li G Inhibition of CD147 (Cluster of Differentiation 147) Ameliorates Acute Ischemic Stroke in Mice by Reducing Thromboinflammation. Stroke 2017, 48 (12), 3356–3365. [PubMed: 29114092]

(13). Jin R; Liu S; Wang M; Zhong W; Li G Inhibition of CD147 Attenuates Stroke-Associated Pneumonia Through Modulating Lung Immune Response in Mice. Front Neurol 2019, 10, 853. [PubMed: 31447768]

(14). Wang S; Liu C; Liu X; He Y; Shen D; Luo Q; Dong Y; Dong H; Pang Z Effects of matrix metalloproteinase inhibitor doxycycline and CD147 antagonist peptide-9 on gallbladder carcinoma cell lines. Tumor Biol. 2017, 39 (10), 1010428317718192.

(15). Zhou J; Zhu P; Jiang JL; Zhang Q; Wu ZB; Yao XY; Tang H; Lu N; Yang Y; Chen ZN Involvement of CD147 in overexpression of MMP-2 and MMP-9 and enhancement of invasive potential of PMA-differentiated THP-1. BMC Cell Biol. 2005, 6 (1), 25. [PubMed: 15904490]

(16). Cuadrado I; Piedras MJ; Herruzo I; Turpin M. e. C.; Castejón B; Reventun P; Martin A; Saura M; Zamorano JL; Zaragoza C EMMPRIN-Targeted Magnetic Nanoparticles for In Vivo Visualization and Regression of Acute Myocardial Infarction. Theranostics 2016, 6 (4), 545–57. [PubMed: 26941847]

(17). Yang Y; Lu N; Zhou J; Chen ZN; Zhu P Cyclophilin A up-regulates MMP-9 expression and adhesion of monocytes/macro-phages via CD147 signalling pathway in rheumatoid arthritis. Rheumatology (Oxford, U. K.) 2008, 47 (9), 1299–310.

(18). Schlegel J; Redzic JS; Porter CC; Yurchenko V; Bukrinsky M; Labeikovsky W; Armstrong GS; Zhang F; Isern NG; DeGregori J; Hodges R; Eisenmesser EZ Solution characterization of the extracellular region of CD147 and its interaction with its enzyme ligand cyclophilin A. J. Mol. Biol 2009, 391 (3), 518–35. [PubMed: 19500591]

(19). Liu S; Li Y; Wang X; Ma J; Zhang L; Xia G Preparation, Characterization, and Antitumor Activities of Miriplatin-Loaded Liposomes. J. Pharm. Sci 2016, 105 (1), 78–87. [PubMed: 26852842]

(20). Liu S; Huang W; Jin MJ; Fan B; Xia GM; Gao ZG Inhibition of murine breast cancer growth and metastasis by survivin-targeted siRNA using disulfide cross-linked linear PEI. Eur. J. Pharm. Sci 2016, 82, 171–82. [PubMed: 26554721]

(21). Liu S; Huang W; Jin MJ; Wang QM; Zhang GL; Wang XM; Shao S; Gao ZG High gene delivery efficiency of alkylated low-molecular-weight polyethylenimine through gemini surfactant-like effect. Int. J. Nanomed 2014, 9, 3567–81.

(22). Benedek A; Móricz K; Jurányi Z; Gigler G; Lévay G; Hársing LG; Mátyus P; Szénási G; Albert M Use of TTC staining for the evaluation of tissue injury in the early phases of reperfusion after focal cerebral ischemia in rats. Brain Res. 2006, 1116 (1), 159–65. [PubMed: 16952339]

(23). Jin R; Song Z; Yu S; Piazza A; Nanda A; Penninger JM; Granger DN; Li G Phosphatidylinositol-3-kinase gamma plays a central role in blood-brain barrier dysfunction in acute experimental stroke. Stroke 2011, 42 (7), 2033–44. [PubMed: 21546487]

(24). Bederson JB; Pitts LH; Tsuji M; Nishimura MC; Davis RL; Bartkowski H Rat middle cerebral artery occlusion: evaluation of the model and development of a neurologic examination. Stroke 1986, 17 (3), 472–6. [PubMed: 3715945]

(25). Moran PM; Higgins LS; Cordell B; Moser PC Age-related learning deficits in transgenic mice expressing the 751-amino acid isoform of human beta-amyloid precursor protein. Proc. Natl. Acad. Sci. U. S. A 1995, 92 (12), 5341–5. [PubMed: 7777509]

(26). Sumii T; Lo EH Involvement of matrix metalloproteinase in thrombolysis-associated hemorrhagic transformation after embolic focal ischemia in rats. Stroke 2002, 33 (3), 831–6. [PubMed: 11872911]

(27). Liu W; Sood R; Chen Q; Sakoglu U; Hendren J; Cetin O; Miyake M; Liu KJ Normobaric hyperoxia inhibits NADPH oxidase-mediated matrix metalloproteinase-9 induction in cerebral microvessels in experimental stroke. J. Neurochem 2008, 107 (5), 1196–205. [PubMed: 18786175]

(28). García-Yébenes I; Sobrado M; Zarruk JG; Castellanos M; Pérez de la Ossa N; Dávalos A; Serena J; Lizasoain I; Moro MA A mouse model of hemorrhagic transformation by delayed tissue plasminogen activator administration after in situ thromboembolic stroke. Stroke 2011, 42 (1), 196–203. [PubMed: 21106952]

(29). Wang X; Tsuji K; Lee SR; Ning M; Furie KL; Buchan AM; Lo EH Mechanisms of hemorrhagic transformation after tissue plasminogen activator reperfusion therapy for ischemic stroke. Stroke 2004, 35 (11 Suppl 1), 2726–30. [PubMed: 15459442]

(30). Jeong WJ; Bu J; Kubiatowicz LJ; Chen SS; Kim Y; Hong S Peptide-nanoparticle conjugates: a next generation of diagnostic and therapeutic platforms? Nano Converg 2018, 5 (1), 38. [PubMed: 30539365]

(31). Li X; Zheng L; Xia Q; Liu L; Mao M; Zhou H; Zhao Y; Shi J A novel cell-penetrating peptide protects against neuron apoptosis after cerebral ischemia by inhibiting the nuclear trans-location of annexin A1. Cell Death Differ. 2019, 26 (2), 260–275. [PubMed: 29769639]

(32). Tu J; Zhang X; Zhu Y; Dai Y; Li N; Yang F; Zhang Q; Brann DW; Wang R Cell-Permeable Peptide Targeting the Nrf2-Keap1 Interaction: A Potential Novel Therapy for Global Cerebral Ischemia. J. Neurosci 2015, 35 (44), 14727–39. [PubMed: 26538645]

(33). Tu TM; Kolls BJ; Soderblom EJ; Cantillana V; Ferrell PD; Moseley MA; Wang H; Dawson HN; Laskowitz DT Apolipoprotein E mimetic peptide, CN-105, improves outcomes in ischemic stroke. Ann. Clin. Transl. Neurol 2017, 4 (4), 246–265. [PubMed: 28382306]

(34). Cho S; Szeto HH; Kim E; Kim H; Tolhurst AT; Pinto JT A novel cell-permeable antioxidant peptide, SS31, attenuates ischemic brain injury by down-regulating CD36. J. Biol. Chem 2007, 282 (7), 4634–42. [PubMed: 17178711]

(35). Hwang H; Jeong HS; Oh PS; Na KS; Kwon J; Kim J; Lim S; Sohn MH; Jeong HJ Improving Cerebral Blood Flow Through Liposomal Delivery of Angiogenic Peptides: Potential of ^{18}F-FDG PET Imaging in Ischemic Stroke Treatment. J. Nucl. Med 2015, 56 (7), 1106–11. [PubMed: 25977466]

(36). Ravasco JMJM; Faustino H; Trindade A; Gois PMP Bioconjugation with Maleimides: A Useful Tool for Chemical Biology. Chem. - Eur. J 2019, 25 (1), 43–59. [PubMed: 30095185]

(37). Weidle UH; Scheuer W; Eggle D; Klostermann S; Stockinger H Cancer-related issues of CD147. Cancer Genomics Proteomics 2010, 7 (3), 157–69. [PubMed: 20551248]

(38). Xu J; Shen ZY; Chen XG; Zhang Q; Bian HJ; Zhu P; Xu HY; Song F; Yang XM; Mi L; Zhao QC; Tian R; Feng Q; Zhang SH; Li Y; Jiang JL; Li L; Yu XL; Zhang Z; Chen ZN A randomized controlled trial of Licartin for preventing hepatoma recurrence after liver transplantation. Hepatology 2007, 45 (2), 269–76. [PubMed: 17256759]

(39). Chen X; Lin J; Kanekura T; Su J; Lin W; Xie H; Wu Y; Li J; Chen M; Chang J A small interfering CD147-targeting RNA inhibited the proliferation, invasiveness, and metastatic activity of malignant melanoma. Cancer Res. 2006, 66 (23), 11323–30. [PubMed: 17145878]

(40). Jin R; Xiao AY; Liu S; Wang M; Li G Taurine Reduces tPA (Tissue-Type Plasminogen Activator)-Induced Hemorrhage and Microvascular Thrombosis After Embolic Stroke in Rat. Stroke 2018, 49 (7), 1708–1718. [PubMed: 29844028]

(41). Dean NR; Newman JR; Helman EE; Zhang W; Safavy S; Weeks DM; Cunningham M; Snyder LA; Tang Y; Yan L; McNally LR; Buchsbaum DJ; Rosenthal EL Anti-EMMPRIN monoclonal antibody as a novel agent for therapy of head and neck cancer. Clin. Cancer Res 2009, 15 (12), 4058–65. [PubMed: 19509148]

(42). Fu ZG; Wang L; Cui HY; Peng JL; Wang SJ; Geng JJ; Liu JD; Feng F; Song F; Li L; Zhu P; Jiang JL; Chen ZN A novel small-molecule compound targeting CD147 inhibits the motility and invasion of hepatocellular carcinoma cells. Oncotarget 2016, 7 (8), 9429–47. [PubMed: 26882566]

(43). Spinello I; Saulle E; Quaranta MT; Pasquini L; Pelosi E; Castelli G; Ottone T; Voso MT; Testa U; Labbaye C The small-molecule compound AC-73 targeting CD147 inhibits leukemic cell proliferation, induces autophagy and increases the chemo-therapeutic sensitivity of acute myeloid leukemia cells. Haematologica 2019, 104 (5), 973–985. [PubMed: 30467201]

(44). Pahk K; Joung C; Song H; Kim S; Kim W A NOVEL CD147 INHIBITOR SP-8356 ATTENUATES PLAQUE PROGRESSION AND STABILIZES VULNERABLE PLAQUE IN APOE-DEFICIENT MICE. J. Hypertens 2019, 37, E105–E106.

(45). Chames P; Van Regenmortel M; Weiss E; Baty D Therapeutic antibodies: successes, limitations and hopes for the future. Br. J. Pharmacol 2009, 157 (2), 220–33. [PubMed: 19459844]

(46). Elgundi Z; Reslan M; Cruz E; Sifniotis V; Kayser V The state-of-play and future of antibody therapeutics. Adv. Drug Delivery Rev 2017, 122, 2–19.

(47). Yang Y; Rosenberg GA Matrix metalloproteinases as therapeutic targets for stroke. Brain Res. 2015, 1623, 30–8. [PubMed: 25916577]

(48). Lakhan SE; Kirchgessner A; Tepper D; Leonard A Matrix metalloproteinases and blood-brain barrier disruption in acute ischemic stroke. Front Neurol 2013, 4, 32. [PubMed: 23565108]

(49). Castellanos M; Leira R; Serena J; Pumar JM; Lizasoain I; Castillo J; Dávalos A Plasma metalloproteinase-9 concentration predicts hemorrhagic transformation in acute ischemic stroke. Stroke 2003, 34 (1), 40–6.

(50). Suzuki Y; Nagai N; Umemura K; Collen D; Lijnen HR Stromelysin-1 (MMP-3) is critical for intracranial bleeding after t-PA treatment of stroke in mice. J. Thromb. Haemostasis 2007, 5 (8), 1732–9. [PubMed: 17596135]

(51). Hafez S; Abdelsaid M; El-Shafey S; Johnson MH; Fagan SC; Ergul A Matrix Metalloprotease 3 Exacerbates Hemorrhagic Transformation and Worsens Functional Outcomes in Hyperglycemic Stroke. Stroke 2016, 47 (3), 843–51. [PubMed: 26839355]

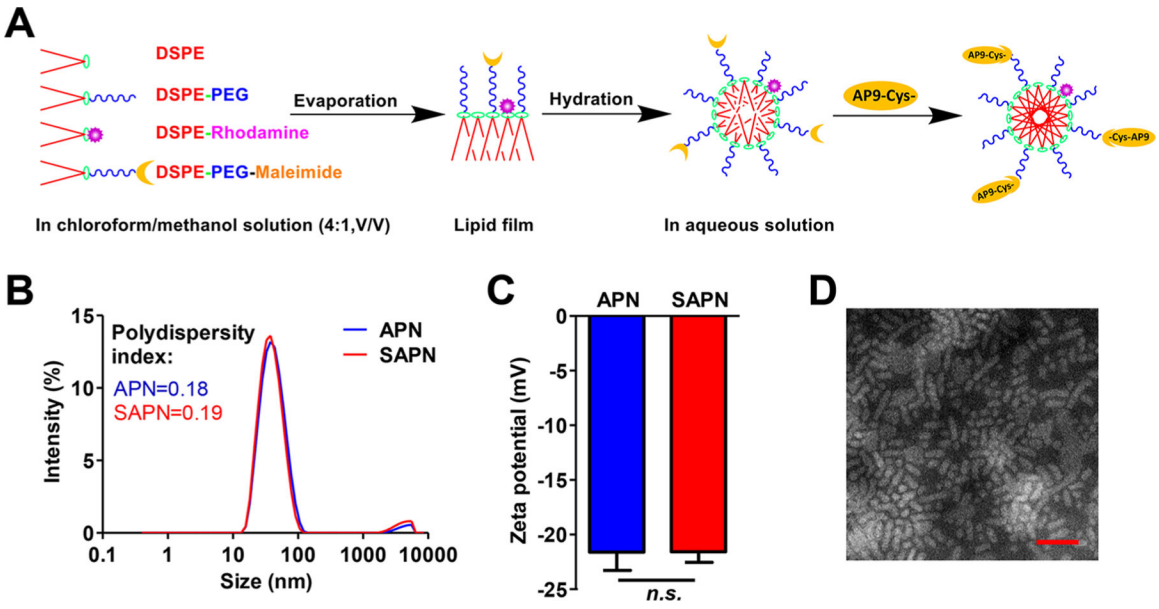

Figure 1.

Preparation and characterization of AP9 conjugated nanoparticles (APN). (A) Scheme for preparing APN using film dispersion method. (B) Particle size distribution and (C) zeta potential of APN. (D) Morphological characteristics of APN detected by transmission electron microscopy (TEM). Scale bar, 100 μm.

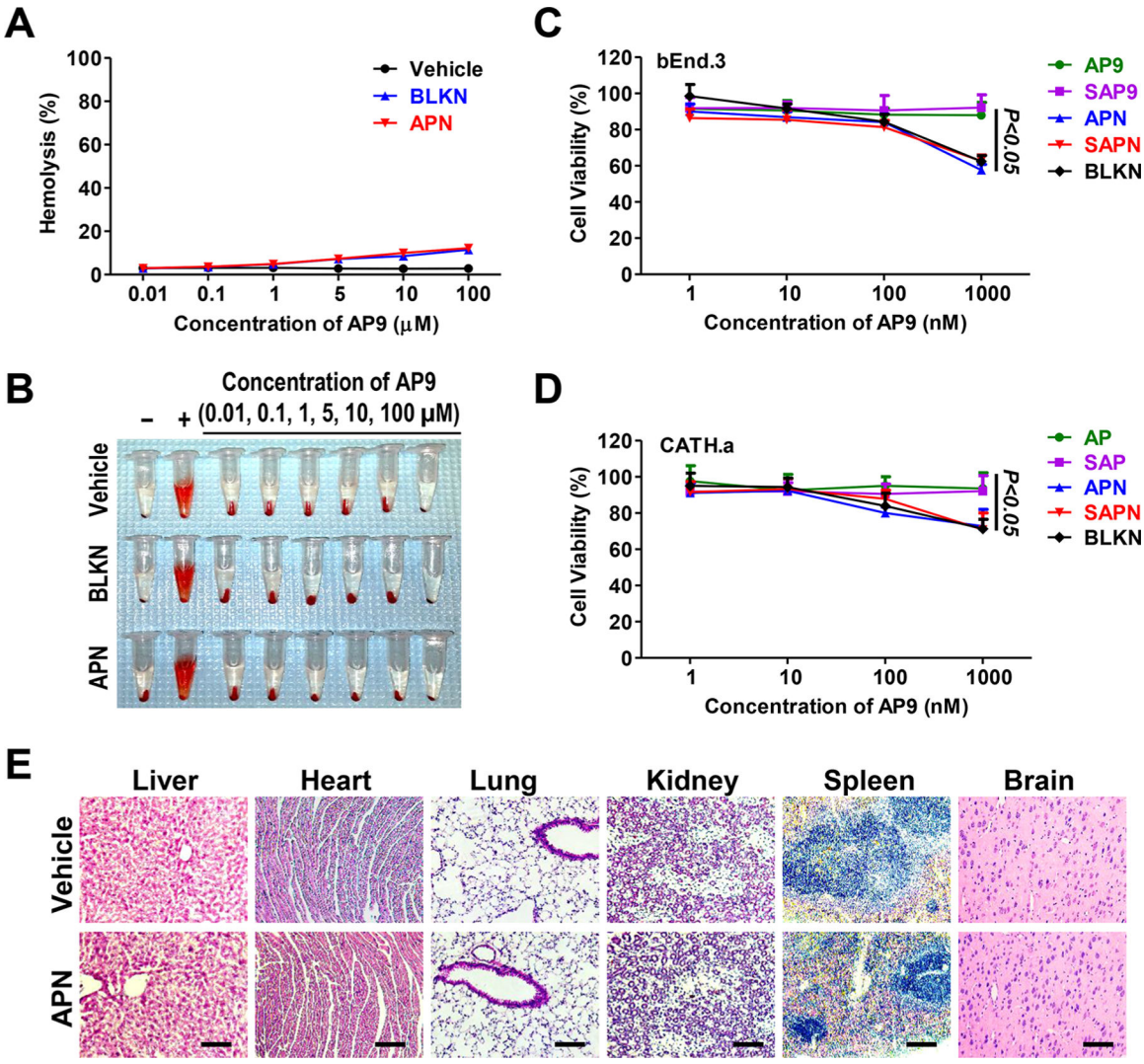

Figure 2.

Blood compatibility, cytotoxicity, and in vivo toxicity of APN. (A) Percentage of hemolysis of RBCs incubated with vehicle, BLKN, and APN at different concentrations ranging from 0.01 to 100 Mm for 1 h at 37 °C. (B) Photographs of hemolysis of RBCs in the presence of vehicle, BLKN, and APN. Distilled water (+) and D-PBS (−) were used as positive and negative control, respectively. (C, D) Cytotoxicity of AP9 (free peptide AP9), SAP9 (scrambled peptide AP9), APN (AP9 conjugated nanoparticles), SAPN (Scrambled AP9 conjugated nanoparticles), and BLKN (Blank nanoparticles) on (C) bEnd.3 and (D) CATH.a cells after 48 h treatment. Data are presented as the mean ± SD. (E) Representative images of HE staining of major organs 3 days after injection of APN at dose of 5 mg/kg in normal mice. Scale bars, 100 μm.

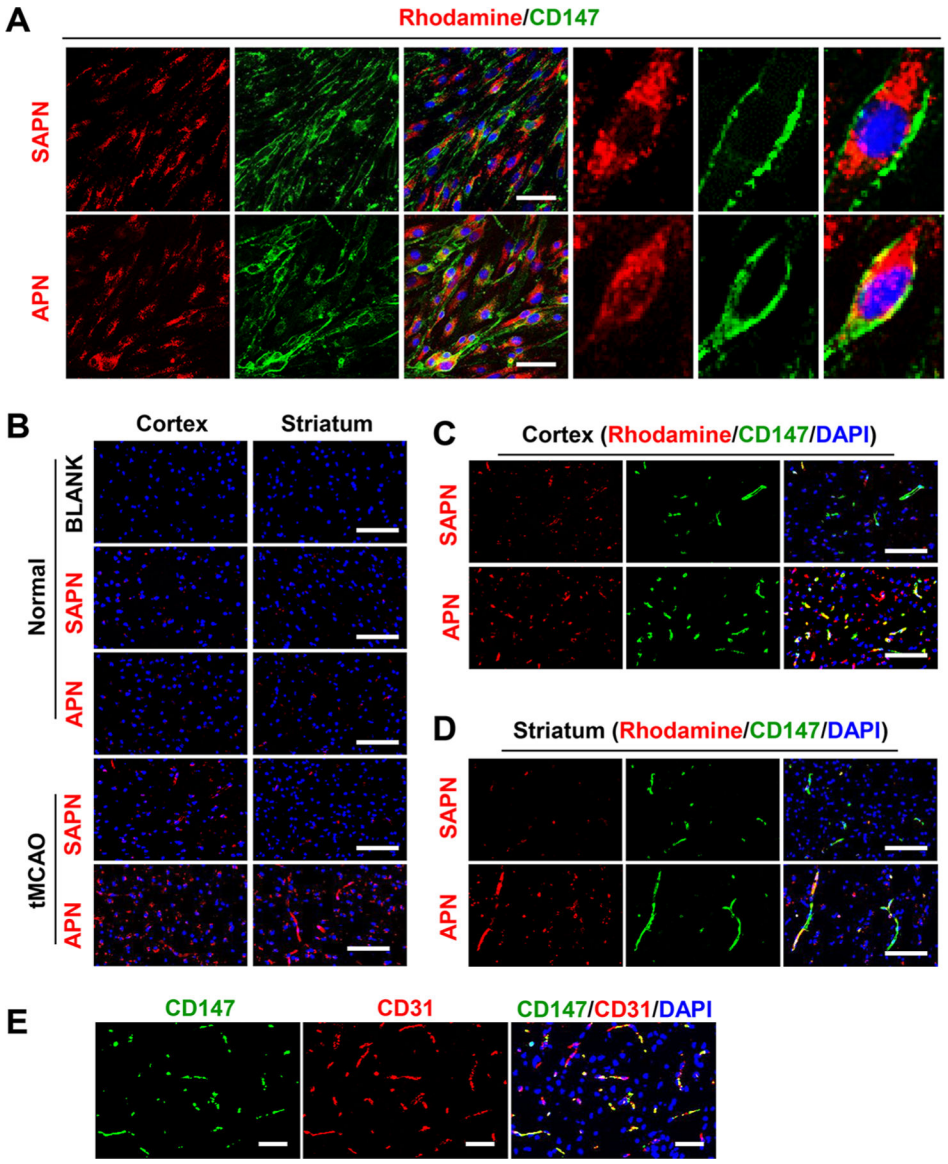

Figure 3.

APN binds to CD147 in vitro and in vivo. (A) Fluorescence images from immunocytochemistry showing that rhodamine-labeled (red) APN, but not SAPN, binds to endogenous CD147 (green) in bEnd.3 cells. Scale bars, 50 μm. (B) Fluorescence images showing that penetration of APN into the cerebral cortex and striatum is increased after tMCAO in mouse. Note that penetration of SAPN in mouse ischemic brain is significantly lower than that of APN. Scale bars, 100 μm. (C, D) Fluorescence images from immunohistochemistry showing that rhodamine-labeled (red) APN, but not SAPN, binds to endogenous CD147 (green) in (C) cerebral cortex and (D) striatum after tMCAO in mouse. Scale bars, 100 μm. (E) Fluorescence images from immunohistochemistry showing that ischemia-induced CD147 colocalized primarily with CD31-labeld microvascular endothelial cells in the ischemic cortex 24 h after stroke. Scale bars, 50 μm.

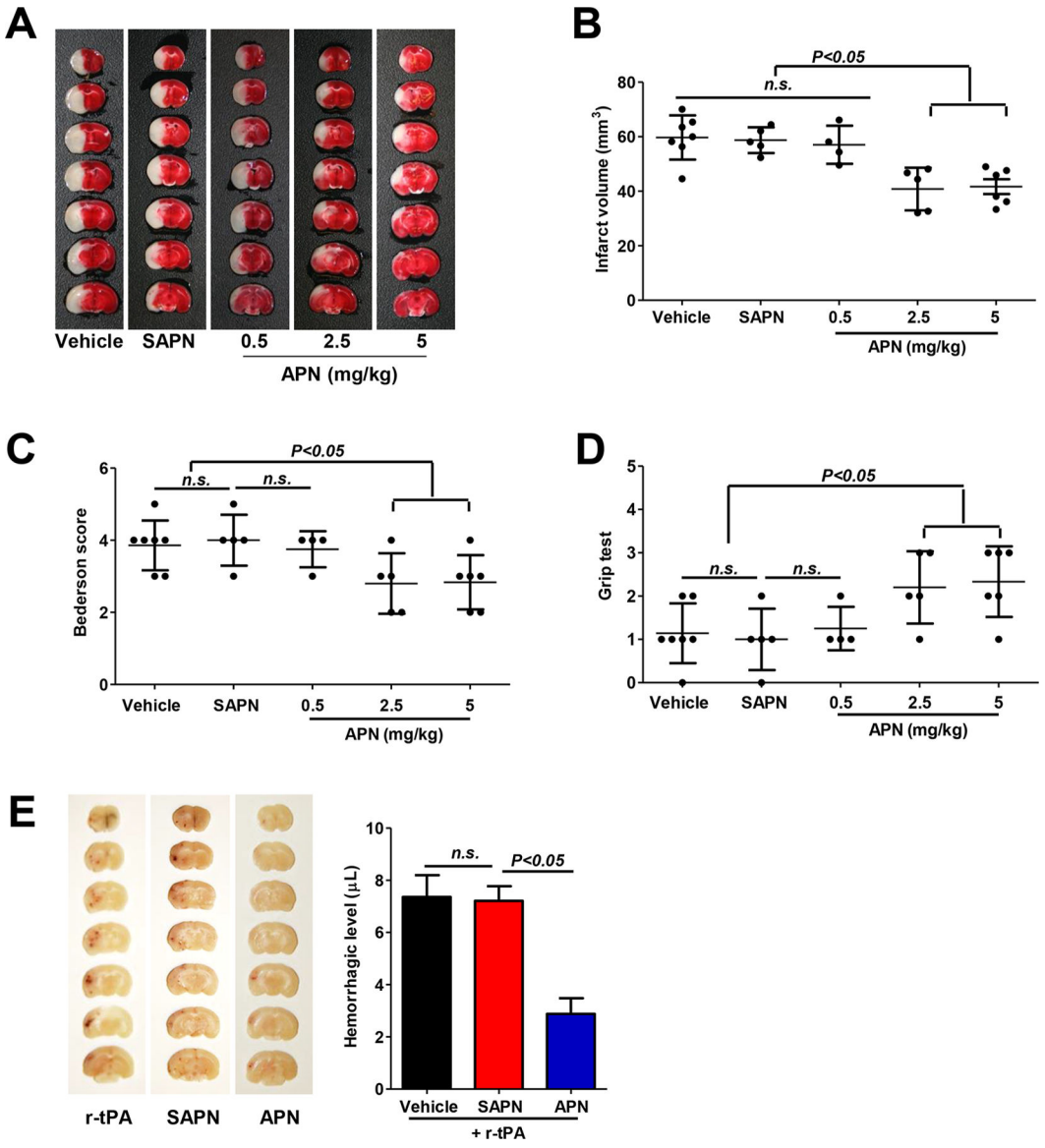

Figure 4.

APN reduces infarct volumes, neurological deficits, and delayed tPA-induced intracerebral hemorrhage after tMCAO in mouse. (A) Representative images of TTC-stained brain coronal sections of mice in indicated groups 3 days after tMCAO. (B) Quantitative analysis of infarct volumes. (C, D) Neurological deficits were evaluated with the (C) Bederson test and the (D) grip test 3 days after tMCAO. n.s. indicates not statistically significant. (E) Representative images of unstained coronal sections (left) showing intracerebral hemorrhage (red color) induced by delayed tPA and quantitative analysis of hemorrhage volume (right) in indicated groups 1 day after tMCAO. n.s. indicates not statistically significant.

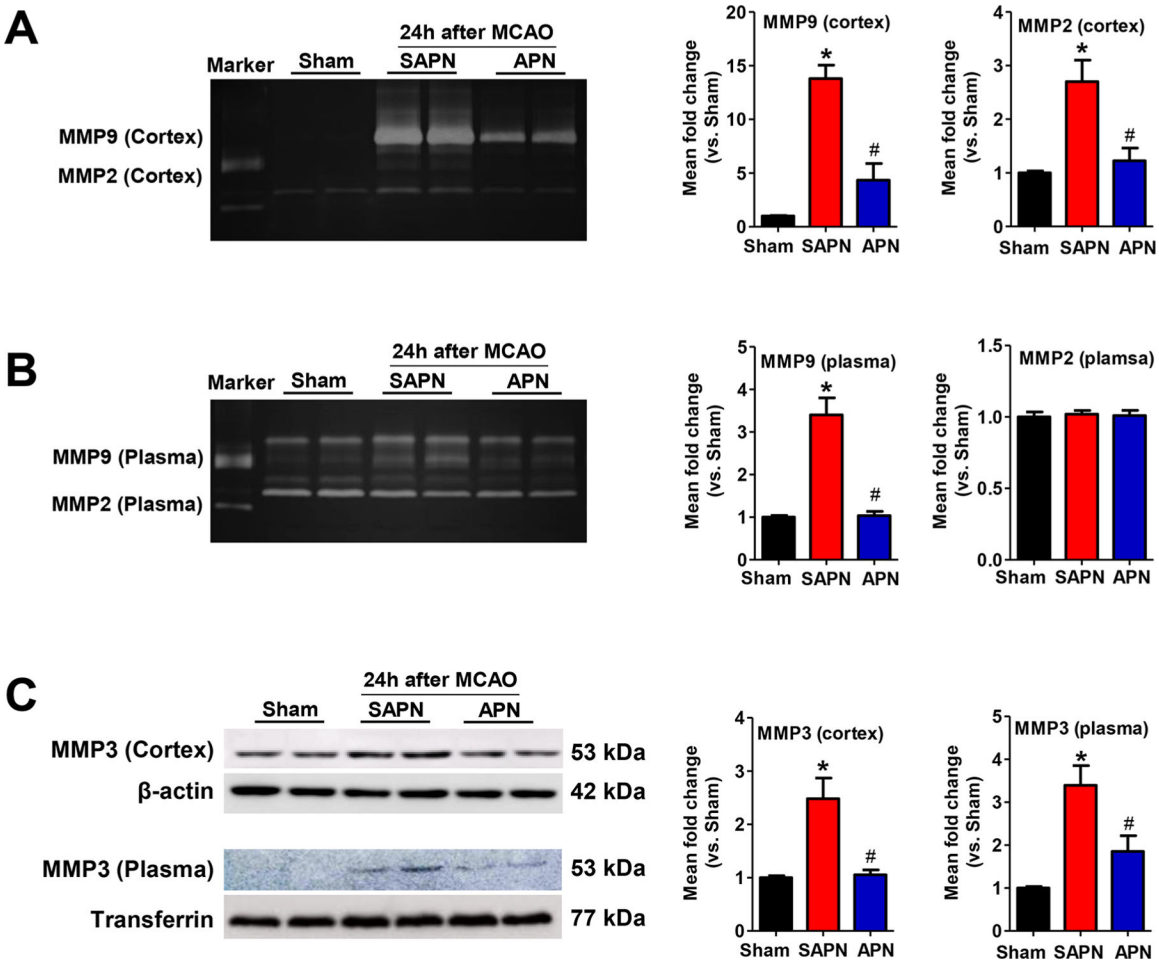

Figure 5.

APN reduces the activity/expression of ischemia-induced cerebral and plasma MMPs. (A, B) Representative images (left) and quantitative analysis (right) of gelatin zymography for MMP-2 and MMP-9 activity in the (A) cerebral cortex and (B) plasma in the indicated groups. Marker: standard human MMP-2/MMP-9 mixed marker. Semiquantification of MMP bands was performed using densitometry. Data are expressed as mean ± SD *, $P < 0.05$ versus Sham; #, $P < 0.05$ versus SAPN. (C) Representative images (left) and quantitative analysis (right) of Western blotting for MMP-3 expression in the cerebral cortex (upper panel) and plasma (lower panel) in the indicated groups. *, $P < 0.05$ versus Sham; #, $P < 0.05$ versus SAPN.